Quantum noise in a laser with nonorthogonal polarization modes

A. M. van der Lee, A. L. Mieremet, M. P. van Exter, N. J. van Druten, and J. P. Woerdman
Huygens Laboratory, Leiden University, P.O. Box 9504, Leiden, The Netherlands
(Received 3 September 1999; published 15 February 2000)

We describe the quantum-noise behavior of a laser that has nonorthogonal polarization modes. The nonorthogonality of the modes leads to excess quantum noise. Theoretically, we derive the excess noise dynamics of the laser, including the saturation of the gain medium. Experimentally, we have measured the noise dynamics in the polarization, intensity and phase degrees of freedom of a 3.51-μm HeXe laser and we obtain good agreement with theory. When the modes are made nonorthogonal we observe: (i) excess intensity and phase noise, (ii) spectral coloring of the excess intensity noise and (iii) correlations between the polarization-angle noise and the intensity noise. The excess phase noise is found to be partly suppressed by the polarization-anisotropic part of the saturation of the gain medium.

PACS number(s): 42.50.Lc, 42.60.Da, 42.55.Lt

I. INTRODUCTION

Spontaneous emission sets a fundamental lower limit to the noise in a laser. This limit corresponds to a noise level of ''one photon per mode'' [1]. It leads for instance to the quantum limit of the laser linewidth, first derived by Schawlow and Townes [2]. The existence of *excess* quantum noise, enhancement of the quantum noise by a factor K relative to the ''one photon per mode'' level, was first predicted by Petermann [3] for gain-guided systems. Subsequently, Siegman [4] showed theoretically that excess noise is a direct consequence of the mode nonorthogonality that is characteristic of open resonators. In addition, he showed that K can reach very large values in unstable-resonator lasers, where the transverse modes are nonorthogonal. The recent experimental demonstration of such very large excess noise factors [5,6] has sparked considerable interest in this phenomenon [7–12].

Recently, it was shown that apart from *longitudinal* or *transverse* laser modes also *polarization* modes can be made nonorthogonal to create excess quantum noise [13–15]. The polarization variant has the advantage that the laser dynamics is restricted to two modes only and hence the situation is inherently more simple than when dealing with a manifold of spatial modes. In addition, in practical lasers the polarization dynamics is relatively slow, so that the nonorthogonal-mode dynamics is easily accessible experimentally. We have used these advantages to demonstrate that excess quantum noise is colored [14].

A quantum derivation of the excess noise factor for a ''toy model'' of a laser that has two modes only was given in Ref. [7]. The case of a laser with two polarization modes considered in the present paper is a realization of a two-mode system. However, this ''toy model'' neglects the nonlinearities in a laser above threshold, which we will show to be of great importance for the excess-noise properties.

In this paper we report a detailed study of the quantum noise in a laser with nonorthogonal polarization modes, extending our previous results of Ref. [14]. We study the output of the laser by measuring the fluctuations in polarization orientation, polarization ellipticity, optical intensity, and optical phase. In addition, we measure correlations between the intensity fluctuations and the polarization-orientation fluctuations, as a function of output power and mode nonorthogonality. The relatively simple dynamics of the polarization fluctuations allows a close comparison with theory. A simple theory, based on a modal analysis of the *linear* cavity modes, can give a first indication of the excess noise and spectral coloring due to mode nonorthogonality. However, we will show that a proper *nonlinear* description of the gain medium, including the saturation, is essential to accurately describe the experimental results. For instance, the excess noise in the optical phase is not correctly predicted by the linear theory, while good agreement is obtained with our extended description.

In this paper we focus on the situation where the two nonorthogonal polarization modes have a difference in loss but equal frequencies. Because of the difference in loss, there is only one lasing mode and one can linearize the nonlinear laser dynamics around steady state. The case of two modes with equal loss but different frequencies has been treated in Ref. [13]. In that case, surprisingly good agreement was found between the experiment and the linear theory. Inclusion of saturation of the gain medium is very difficult in this case of *two* lasing modes, and we only discuss it briefly here [see the discussion after Eq. (13)].

The experiments are performed close to threshold, in the regime where the spontaneous-emission noise is dominant. This also means that the measured intensity-noise levels are still well above the shot-noise limit [16].

The outline of the paper is the following. In Sec. II, we briefly summarize the derivation of the excess noise factor associated with the linear anisotropies of the cavity; next we extend the model, by including the nonlinearity of the gain medium, and derive equations describing the power spectra of the quantities of interest. Section III contains the description of the experimental set-up to measure the various noise spectra. In Sec. IV, the experimental results are shown and Sec. V contains the concluding discussion. In the Appendix, we derive the equations that were used to analyze the measured (polarization) noise signals.

II. THEORY

A. Linear mode analysis

Excess quantum noise is associated with nonorthogonal modes, which in our case are nonorthogonal *polarization* modes. In Ref. [13], we showed how the introduction of linear dichroism (difference in loss between orthogonal linear polarizations) in combination with circular birefringence (difference in refractive index between σ_+ and σ_- modes) in the cavity leads to nonorthogonal polarization modes [an alternative way to produce nonorthogonal polarization modes is to use linear birefringence and linear dichroism at 45° (Ref. [15])]. We will review here briefly the polarization properties of the laser neglecting the nonlinearity of the gain medium. These can be described using the Jones matrix formalism,

$$\frac{d}{dt}\vec{E} = M\vec{E} + \vec{f}, \tag{1}$$

where $\vec{E}$ is a two-component complex-valued vector, describing the polarization state of the light in the cavity, M is a 2×2 Jones matrix and $\vec{f}$ is the Langevin noise source describing spontaneous emission; $\vec{f}$ is taken to be polarization-isotropic. In our experiment we have circular birefringence and linear dichroism in the cavity. The circular birefringence Ω leads to a detuning of the two circularly polarized modes and the linear dichroism $A>0$ induces dissipative coupling between the two circularly polarized states. This leads to the following form of Eq. (1) in a σ_+, σ_- basis

$$\frac{d}{dt}\begin{pmatrix} E_+ \\ E_- \end{pmatrix} = \begin{pmatrix} i\Omega & -A \\ -A & -i\Omega \end{pmatrix}\begin{pmatrix} E_+ \\ E_- \end{pmatrix} + \begin{pmatrix} f_+ \\ f_- \end{pmatrix}, \tag{2}$$

where E_+ and E_- are the slowly varying amplitudes of the σ_+ and σ_--polarized light, respectively. The complex-valued Langevin noise sources f_+ and f_- have uncorrelated real and imaginary parts and obey

$$\langle f_i^*(t) f_j(t')\rangle = R_{\mathrm{sp}}\delta_{ij}\delta(t-t'), \quad \text{for } (i,j=+,-), \tag{3}$$

where R_{sp} is the spontaneous emission rate into each optical mode. The eigenvectors of the matrix M give the polarization eigenmodes of the resonator. The real and imaginary part of its eigenvalues give their damping rates and corresponding frequencies (relative to the carrier frequency), respectively. Specifically, the eigenvalues are $\lambda_{1,2} = \pm\sqrt{A^2-\Omega^2}$. When $|\Omega|<A$ the eigenmodes have the same frequency, but different losses. As the frequencies are the same, we call this the locked regime, in analogy to the frequency-locking in a ring-laser gyro [17]. When $|\Omega|>A$, the losses are the same, but the eigenfrequencies differ; we call this the unlocked regime.

The exact behavior of the eigenvalues is depicted in Fig. 1, where the dashed and solid curves give the losses and frequencies of the eigenmodes, respectively. Also the polarization ellipses of the eigenmodes are indicated. In the locked regime, the polarizations of the eigenmodes are linear, whereas in the unlocked regime the polarizations are elliptical with the same main axis but opposite helicity. Figure 1 also shows that the modes become more and more identical (i.e., more and more nonorthogonal) when $|\Omega|$ approaches A. In the linear description used in this subsection, the excess noise that results from this nonorthogonality can be obtained in two different ways.

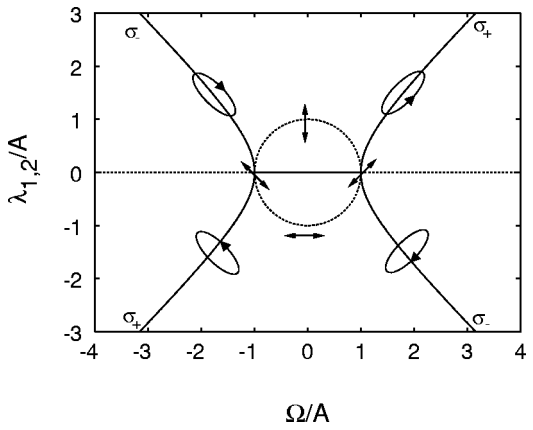

FIG. 1. The normalized relative frequency (solid line) and damping (dashed line) of the eigenmodes of the cavity as function of Ω/A. The polarization states of the eigenmodes are also indicated.

The usual approach, as pioneered by Siegman [4] for a laser with nonorthogonal transverse modes, is to rewrite Eq. (1) into the basis of its (generally nonorthogonal) eigenvectors. The required nonunitary basis transformation diagonalizes the matrix M, but leads to correlated noise sources f_1 and f_2,

$$\frac{d}{dt}\begin{pmatrix} E_1 \\ E_2 \end{pmatrix} = \begin{pmatrix} \lambda_1 & 0 \\ 0 & \lambda_2 \end{pmatrix}\begin{pmatrix} E_1 \\ E_2 \end{pmatrix} + \frac{1}{\sin\alpha}\begin{pmatrix} f_1 \\ f_2 \end{pmatrix}, \tag{4}$$

where 2α is the angle between the polarization eigenmodes on the Poincaré sphere [18]; in our case $\cos\alpha = |\Omega/A|$ when $|\Omega|<A$ and $\cos\alpha = |A/\Omega|$ when $|\Omega|>A$. Note that $\cos\alpha = 0$ for orthogonal modes and $\cos\alpha = 1$ for parallel (i.e., maximally nonorthogonal) eigenmodes. The correlated noise sources in Eq. (4) obey

$$\begin{aligned} \langle f_1^*(t) f_1(t')\rangle &= \langle f_2^*(t) f_2(t')\rangle = R_{\mathrm{sp}}\delta(t-t'), \\ \langle f_1^*(t) f_2(t')\rangle &= R_{\mathrm{sp}}\delta(t-t')\cos\alpha. \end{aligned} \tag{5}$$

In this framework the standard argument [4] to explain the appearance of the excess quantum noise is as follows: when one eigenmode has less loss than all other eigenmodes (in our case when $|\Omega|<A$), the lowest-loss eigenmode will be the lasing mode, which has its loss compensated by the gain medium. The assumption in the standard argument is that the laser is effectively single mode and that the nonlasing modes can be neglected. Thus the laser mode can be thought of as being independently driven by a noise source with a diffusion coefficient that is enhanced by a factor $\sin^{-2}\alpha$. The excess noise factor is then given by

$$K = \frac{1}{\sin^2\alpha} = \frac{A^2}{A^2-\Omega^2}. \tag{6}$$

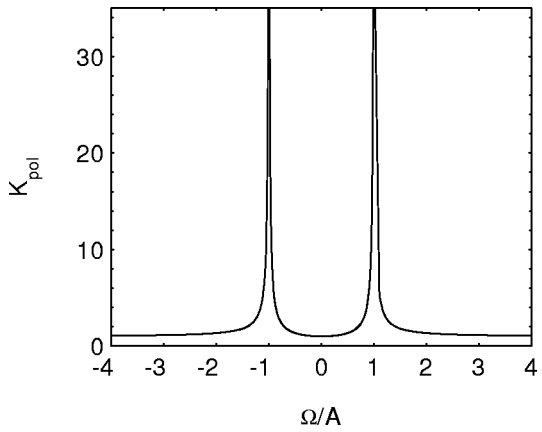

FIG. 2. The excess noise factor, K_{pol} as function of Ω/A. Note that K_{pol} increases as the two eigenmodes become more nonorthogonal at $\Omega/A \rightarrow 1$.

Within this linear description the enhancement factor is expected to multiply both the intensity noise and the phase noise. Note that K diverges for $|\Omega| \rightarrow A$; in this limit the polarization eigenmodes become degenerate. The behavior of the K factor as a function of Ω/A is plotted in Fig. 2.

An alternative description of excess noise is obtained when using a unitary basis transformation to rewrite Eq. (1) into an orthogonal basis that contains eigenmode 1 and a perpendicular mode b (not an eigenmode), to obtain [7]

$$\frac{d}{dt}\begin{pmatrix} E_1 \\ E_b \end{pmatrix} = \begin{pmatrix} \lambda_1 & (\lambda_1 - \lambda_2)\sqrt{K-1} \\ 0 & \lambda_2 \end{pmatrix}\begin{pmatrix} E_1 \\ E_b \end{pmatrix} + \begin{pmatrix} f_1 \\ f_b \end{pmatrix}. \tag{7}$$

In this orthogonal basis the noise sources f_1 and f_b are uncorrelated and have equal strength, but the dynamical evolution is such that fluctuations in the b mode partially project into mode 1, since matrix M is now triangular. This alternative description gives a simple explanation for the appearance of excess noise: it originates through projection from fluctuations in the other modes [note the factor $\sqrt{K-1}$ in the off-diagonal matrix element in Eq. (7)]. It also shows that the excess noise has certain dynamics which is related to the modal dynamics and eigenvalues, leading to the spectral coloring of the excess noise [14].

Both approaches are easy to perform in two-mode context, but in a many-mode context the first approach [leading to Eq. (4)] is more suitable to calculate the magnitude of the excess noise, as the K factor of the lasing mode appears directly in the strength of its noise source [4]. The second approach [leading to Eq. (7)] shows better the origin of the dynamics of the excess noise and, as it uses an orthogonal basis, this method is suitable for a quantum description of excess noise [7,8].

B. Including the gain medium

We now extend the above analysis, and include the nonlinearities of the gain medium by using a vector extension of Lamb's third-order scalar theory [19] and include Langevin noise sources to take into account the effect of quantum noise. This gives the following semi-classical equations for the two amplitudes E_+ and E_- of the $\sigma+$ and σ_- polarization modes

$$\frac{d}{dt}E_+ = (g - \beta_s I_+ - \beta_c I_-)E_+ + i\Omega E_+ - AE_- + f_+, \tag{8a}$$

$$\frac{d}{dt}E_- = (g - \beta_s I_- - \beta_c I_+)E_- - i\Omega E_- - AE_+ + f_-, \tag{8b}$$

where g is the linear isotropic net gain, β_s is the self-saturation coefficient and β_c the cross-saturation coefficient. $I_\pm = |E_\pm|^2$ represents the intensity of the $\sigma_\pm$ mode. We restrict the discussion to a single-frequency laser tuned to gain maximum so that g is real and the saturation coefficients are real (i.e. nonlinear dispersion is absent). Equation (8) corresponds to a class-A laser [20]; i.e., it assumes that the inversion dynamics is sufficiently fast that it may be adiabatically eliminated. In the experiments, we observe clearly resolved relaxation oscillations, indicating that the inversion dynamics can in fact not be adiabatically eliminated (class-B laser). Nevertheless, a class-A description turns out to be sufficient, since the polarization dynamics occurs at frequencies that are considerably smaller than the relaxation oscillation frequency (typically 2 MHz versus 15 MHz) [21, 22]

The quantum noise sources in Eq. (8) have been collected into $f_\pm$. In principle a Langevin noise source corresponds to each gain and loss term in this equation in accordance with the fluctuation-dissipation theorem. As we assume to be close to threshold we neglect the influence of noise in the inversion on the intensity. Furthermore, we assume that the polarization-independent loss is much larger than the polarization dependent loss, thus the noise sources f_+ and f_- are approximately equally strong and uncorrelated. With these approximations spontaneous emission is the dominant noise source, and we may use Eq. (3) for f_+ and f_-, both in Eqs. (8) and (2).

Because of the nonlinear nature of Eqs. (8), dealing with the complex-valued field amplitudes becomes awkward. Instead, we can rewrite the two complex-valued Eqs. (8) into four real-valued equations, by separating the complex electric fields in a real amplitude and a phase ($E_+ = \mathcal{E}_+ e^{i\phi_+}$). It is convenient to express these equations in the four experimental quantities: the polarization angle θ ($\theta = 0$ when the principal axis of the polarization ellipse is aligned along the high loss axis of the dichroism, A), the ellipticity angle χ, the intensity I, and the optical phase ϕ,

$$\theta = \frac{\phi_+ - \phi_-}{2}, \tag{9a}$$

$$\tan\chi = \frac{\mathcal{E}_- - \mathcal{E}_+}{\mathcal{E}_+ + \mathcal{E}_-}, \tag{9b}$$

$$I = \mathcal{E}_+^2 + \mathcal{E}_-^2, \tag{9c}$$

$$\phi = \frac{\phi_+ + \phi_-}{2}. \tag{9d}$$

The following equations are obtained [23]

$$\frac{1}{2I}\frac{d}{dt}I = -A\cos 2\,\theta\cos 2\chi + g - \beta_s I + \frac{\beta_s - \beta_c}{2} I\cos^2 2\chi + f_{\tilde{I}}, \tag{10a}$$

$$\frac{d}{dt}\theta = \Omega + \frac{A}{\cos 2\chi}\sin 2\theta + f_\theta, \tag{10b}$$

$$\frac{d}{dt}\phi = A\tan 2\chi \sin 2\theta + f_\phi, \tag{10c}$$

$$\frac{d}{dt}\chi = A\cos 2\theta \sin 2\chi - \frac{1}{4}(\beta_s - \beta_c) I \sin 4\chi + f_\chi. \tag{10d}$$

The Langevin noise sources in the above equation are characterized by the following correlation functions:

$$\langle f_i(t) f_j(t')\rangle = A_i D \delta_{ij}\delta(t-t'), \tag{11a}$$

$$A_{\tilde{I}} = A_\chi = 1, \tag{11b}$$

$$A_\phi = A_\theta = \frac{1}{\cos^2 2\chi}, \tag{11c}$$

where $D = R_{sp}/2I$. We note that there are no cross correlations between the different Langevin noise sources, so the noise sources are independent.

From Eqs. (10) we can derive the stationary solutions (I_0, θ_0, χ_0) by setting the time derivatives equal to zero and neglecting the noise sources. For $|\Omega| < A$, this leads to

$$I_0 = \frac{2(g - A\cos 2\theta_0)}{\beta_s + \beta_c}, \tag{12a}$$

$$\sin 2\theta_0 = -\Omega/A, \tag{12b}$$

$$\chi_0 = 0. \tag{12c}$$

The overall optical phase, ϕ, of the laser is undetermined. In the locked regime, the stationary polarization states (θ_0 and χ_0) are not changed by the inclusion of the gain medium, and are the same as for the eigenmodes in the linear analysis. The stationary states are linearly polarized ($\chi_0 = 0$), and it can be seen that the polarization angle has two solutions, a stable and an unstable solution corresponding to the lasing and nonlasing eigenmodes found in the linear analysis of Sec. II A.

When $|\Omega| > A$, we are in the unlocked regime, where there is no longer a stable polarization state. The polarization angle of the laser will follow a nonuniform rotation making the full problem of the four coupled Eqs. (10) very difficult. When we can neglect the variations in the intensity (laser far enough above threshold), and assume that the polarization-anisotropic saturation forces the polarization of the laser to be linear ($\beta_s - \beta_c > 0$), the rotation of the polarization angle can be derived from Eqs. (10), leading to the Adler equation,

$$\frac{d}{dt}\theta = \Omega + A\sin 2\theta + f_\theta. \tag{13}$$

The properties of this equation, including the noise source f_θ, have been theoretically investigated by Cresser *et al.* [24] in the context of a laser gyro.

In Ref. [13], we have measured the quantum noise of a laser in the unlocked regime ($|\Omega| > A$). The observed excess quantum noise could be explained surprisingly well with a linear mode analysis. The effects of the nonlinear saturation, as incorporated in the Adler equation, only lead to a small correction of the linear result [13]. Further analysis of the unlocked regime, beyond what is already present in Refs. [13] and [24], seems prohibitively difficult and we do not attempt it here. This difficulty is due to the presence of two eigenmodes that lase simultaneously in combination with the nonlinearity of the gain medium. If, in some way, the laser would be forced to lase in only one of the two linear eigenmodes (for instance if the gain medium would be spectrally narrow enough to select only one mode) the problem could be treated in the same manner as in the locked regime. Also other theories describe excess noise only in a single-lasing-mode context [4,8]. In our experiments we will only use the *deterministic* part of the dynamics in the unlocked regime, since this offers a diagnostic method to derive the values of Ω and A (see Sec. IV A).

Returning now to the locked regime $|\Omega| < A$, we linearize around the stable steady state, i.e., we write $I = I_0(1 + 2\delta\tilde{I})$, $\theta = \theta_0 + \delta\theta$, $\chi = \chi_0 + \delta\chi$. Substitution in Eq. (10) leads to the following equations:

$$\frac{d}{dt}\delta\tilde{I} = -2\beta_i I_0 \delta\tilde{I} - 2\Omega\,\delta\theta + f_{\tilde{I}}, \tag{14a}$$

$$\frac{d}{dt}\delta\theta = -\gamma\delta\theta + f_\theta, \tag{14b}$$

$$\frac{d}{dt}\phi = -2\Omega\,\delta\chi + f_\phi, \tag{14c}$$

$$\frac{d}{dt}\delta\chi = -(\gamma + 2\beta_a I_0)\delta\chi + f_\chi. \tag{14d}$$

In these equations we have introduced the difference between the loss rates of the lasing and nonlasing modes $\gamma = 2\sqrt{A^2 - \Omega^2}$, the polarization-isotropic saturation coefficient $\beta_i = (\beta_s + \beta_c)/2$ and the polarization anisotropic saturation coefficient $\beta_a = (\beta_s - \beta_c)/2$. Since $\chi_0 = 0$, the Langevin noise sources have now identical diffusion constants [see Eqs. (11)]. For orthogonal polarization modes ($\Omega = 0$) the system simplifies further into four decoupled equations, and all four laser parameters, $\delta\tilde{I}, \delta\theta, \delta\chi, \phi$, are driven only by their respective noise sources. For nonorthogonal polariza-

tion modes, the four equations separate into two subsets of two coupled equations; polarization-angle fluctuations $\delta\theta$ are coupled into the intensity fluctuations $\delta\tilde{I}$, and ellipticity fluctuations $\delta\chi$ enter into the phase fluctuations ϕ. In fact Eqs. (14) are closely analogous to Eq. (7). The variables ($\delta\tilde{I}$, $\delta\theta$, ϕ, $\delta\chi$) are orthogonal, the noise sources are uncorrelated, and the excess noise appears because noise in the orthogonal direction ($\delta\theta$, $\delta\chi$) couples into the lasing mode ($\delta\tilde{I}$, ϕ). The essential difference between Eqs. (7) and (14) is that the latter is obtained after including the nonlinearity of the gain medium and linearization around the steady state. Thus, Eqs. (14) explicitly include the saturation dynamics (through β_i and β_a).

The physical mechanism of the coupling leading to excess quantum noise can be understood as follows. When the polarization eigenmodes are nonorthogonal, the steady-state polarization angle is not aligned with the principal axis of the linear dichroism. As a consequence, polarization-angle fluctuations result in a modulation of the net losses, leading to intensity fluctuations. The misalignment angle is given by $\sin 2\theta = -\Omega/A$ [Eq. (12b)], from which follows that the projection of polarization noise into intensity noise is given by $2A\,\delta\theta \sin 2\theta = -2\Omega\,\delta\theta$ [see Eq. (14a)]. Similarly, the ellipticity fluctuations are converted to phase noise by the circular birefringence. This strength is also determined by the nonorthogonality of the modes [see Eq. (10c)] and leads to the term $-2\Omega\,\delta\chi$.

Taking the Fourier transform of Eq. (14) and calculating the noise power spectra of the four variables results in:

$$\langle|\delta\tilde{I}(\omega)|^2\rangle = \frac{D}{(2\beta_i I_0)^2+\omega^2}\left[1+\frac{4\Omega^2}{\gamma^2+\omega^2}\right], \tag{15a}$$

$$\langle|\delta\theta(\omega)|^2\rangle = \frac{D}{\gamma^2+\omega^2}, \tag{15b}$$

$$\langle|\phi(\omega)|^2\rangle = \frac{D}{\omega^2}\left[1+\frac{4\Omega^2}{(\gamma+2\beta_a I_0)^2+\omega^2}\right], \tag{15c}$$

$$\langle|\delta\chi(\omega)|^2\rangle = \frac{D}{(\gamma+2\beta_a I_0)^2+\omega^2}. \tag{15d}$$

The excess quantum noise is identified with the last terms in the brackets in the equations for the intensity and phase noise [Eqs. (15a) and (15c)]. We now discuss some aspects of the excess noise terms. Firstly, the excess noise is frequency-dependent or colored, as first discussed in Ref. [14]. The origin of this frequency dependence lies in the polarization dynamics. Secondly, we can compare the excess noise derived in this section (i.e. including the nonlinearity of the gain medium) to the prediction of the linear mode analysis of Sec. II A. For that we take the ratio of the noise at $\Omega=0$ (orthogonal modes) and the noise observed at $\Omega\neq 0$, at zero frequency ($\omega\to 0$). In this way we calculate the excess noise factor, *K*, both for the intensity and the phase noise. The enhancement of the intensity noise is

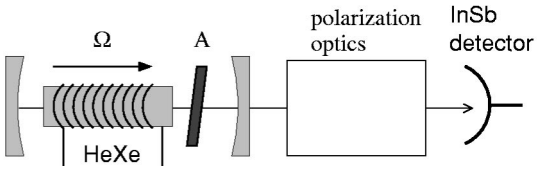

FIG. 3. A schematic picture of the setup. The laser cavity contains a quasi Brewster-plate and coils are used to create an axial magnetic field. The output of the laser can be routed through suitable polarization optics to measure polarization-noise signals. The resulting intensity of the transmitted light is measured with a cryogenic InSb detector.

$$K_I = 1+\frac{\Omega^2}{A^2-\Omega^2} = \frac{A^2}{A^2-\Omega^2}, \tag{16}$$

which is the same as the excess noise factor following from linear mode analysis in Sec. II A, Eq (6).

In contrast, when we calculate the enhancement of the phase noise we find

$$K_\phi = 1+\frac{\Omega^2}{[\sqrt{A^2-\Omega^2}+(\beta_a I)]^2}, \tag{17}$$

i.e., less than expected from the linear mode analysis. The origin of this deviation lies in the suppression of the ellipticity noise by the polarization-anisotropic saturation, $\beta_a I$, which in turn results in a reduction of the excess phase noise. Note that the enhancement of the phase noise depends on how far the laser is above threshold.

Equations (14) also imply a third consequence of the mode nonorthogonality, namely correlations between the intensity fluctuations and polarization-angle fluctuations, and between the phase and ellipticity fluctuations. As reported in Sec. IV, we have measured correlations between the intensity and polarization angle. To describe these theoretically, we need power spectra of the form $\langle|c_1\delta\tilde{I}(\omega)+c_2\delta\theta(\omega)|^2\rangle$, for various real-valued constants c_1 and c_2 (see also Appendix A). For the correlation term in these power spectra we find:

$$\langle\delta\tilde{I}^*(\omega)\,\delta\theta(\omega)\rangle = 2\Omega\frac{D}{(\gamma^2+\omega^2)(2\beta_i I_0+i\omega)}. \tag{18}$$

The magnitude of this correlation depends on the nonorthogonality of the eigenmodes via Ω and γ. For orthogonal modes ($\Omega=0$) the correlation is zero, but when the modes become nonorthogonal ($\Omega\to A$), the correlation increases. In addition, this correlation depends on the output power, via the $\beta_i I_0$ term; for higher output powers the correlation gets smaller. This is due to the fact that the intensity noise is reduced by the saturation and the polarization-angle noise is not.

III. EXPERIMENTAL SET-UP

The experiments were performed using a miniature HeXe gas laser (see Fig. 3). The laser has a stable-cavity configuration consisting of a 60-cm concave gold mirror and a

30-cm concave dielectric outcoupling mirror with a reflectivity of $R=32\%$; the mirrors are separated by a distance of 7 cm. The HeXe gas was RF excited and operated at a pressure of 2 kPa. The 5 cm-long, 1.8-mm inner-diameter gas capillary containing the gas mixture was terminated by two 0.5 mm-thick Infrasil windows having 92% transmission each.

The laser output is split by a 20–80 % beamsplitter of which the 20% part is directed to a large area InAs detector to calibrate the output power and the 80% part is used to measure the noise spectra on a cryogenic InSb detector. The detector is connected to a home-built low-noise amplifier. This combination has a noise level of 1 $\mathrm{pW}/\sqrt{\mathrm{Hz}}$ and a bandwidth of 11 MHz. The electronic signal of the amplifier is fed into an RF-spectrum analyzer, which produces the noise spectra. The frequency resolution of the presented spectra is determined by the resolution-bandwidth used (either 30 kHz or 100 kHz).

To introduce the polarization anisotropies in the cavity, we make use of an axial magnetic field and a tilted CaF_2 plate. The axial magnetic field induces Faraday rotation in the gas medium and leads to circular birefringence in the cavity (Ω). The tilted CaF_2 plate introduces linear dichroism (A) through the difference in reflection of *s*- and *p*-polarized light. In the experiment we normally keep the angle of the tilted CaF_2 plate constant and change the current through the coils generating the magnetic field to modify the nonorthogonality of the cavity modes (as the nonorthogonality depends on the ratio of Ω and A).

By inserting polarization-optical elements (such as a quarter-waveplate and a rotatable polarizer) between the laser and the detector, we can measure polarization-angle fluctuations, ellipticity fluctuations and correlations between the intensity and polarization-angle fluctuations. In practice, instead of a rotatable polarizer we used a fixed optical isolator as a polarizer, in order to eliminate feedback from the detector into the laser, in combination with a rotatable half-waveplate.

Typically the laser was operated $5-50\,\%$ above threshold, yielding output powers around $5-50\ \mu\mathrm{W}$. Also taking into account the effect of the incomplete inversion [27], we expect intensity-noise levels that are one to two orders of magnitude above the shot-noise limit, in agreement with the experimental observations.

To measure the quantum fluctuations in the optical phase, we use an interferometric method to convert the phase noise into intensity noise, namely self-heterodyning [25] (see Fig. 4). Schematically the self-heterodyne setup consists of Mach-Zehner-type interferometer where the laser beam is split in two; one beam is shifted in frequency by an amount of 5-10 MHz by using two acousto-optic modulators (AOMs) in series (one shifting 40 MHz up, the other shifting 35-30 MHz down). The other beam is delayed by letting it propagate through an optical delay line; this beam bounces back and forth between two curved mirrors that are spaced 2 meters, tracing a path length of 180 m. The two beams are recombined and the interference signal at the difference frequency is detected. The variation of the phase of the delayed beam with respect to that of the undelayed beam results in phase variations of the beat signal. This can be measured with the RF spectrum analyzer and yields the amount of optical phase diffusion [25]. We have added an optical isolator behind the laser to eliminate feedback and to avoid that polarization fluctuations influenced the self-heterodyne signal.

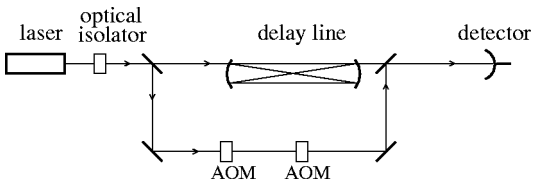

FIG. 4. A schematic picture of the self-heterodyne setup. The output of the laser passes an optical isolator and is split in two. One part is sent through an optical delay line. The other part is shifted 5-10 MHz up in frequency by a combination of two acouto-optic modulators (AOM's). At the end the two beams are recombined and the fluctuations at the beat frequency are measured.

IV. RESULTS

The presentation of the experimental results in this section has been organized in the following way. In Sec. IV A, we start with the method used to determine Ω and A, as these are the crucial parameters defining the nonorthogonality of the eigenmodes. We check the dependence of the steady-state polarization on the applied magnetic field in Sec. IV B. Next, Sec. IV C describes the measurements of the noise in the polarization parameters, θ and χ. Following that, the effects of the nonorthogonality of the cavity modes are discussed: in Sec. IV D the excess quantum noise in the intensity noise, in Sec. IV E the correlations between the intensity and the polarization-angle noise, and in Sec. IV F the excess phase noise.

A. Calibration of Ω and A

The excess intensity noise depends sensitively on the nonorthogonality of the eigenmodes, which is determined by the ratio Ω/A. Thus, it is important to know the values of Ω and A, and in particular that of Ω/A. For this we use the fact that the polarization of the laser output rotates when the magnetic-field-induced circular birefringence is larger than the linear dichroism ($\Omega>A$). In this regime the anharmonic rotation of the polarization angle is described by the Adler equation [Eq. (13)]. We measure this rotation rate by placing a polarizer in the laser beam, and detecting the principal frequency of the resulting intensity modulation [13].

Figure 5 shows the result of a series of such measurements. Here, the intensity modulation frequency, ω_{rot}, is plotted as function of the applied current through the coils, I_B. Fitting the experimental data to the expected relation $\omega_{\mathrm{rot}}=2\sqrt{(aI_B+\Omega_0)^2-A^2}$ gives us both the circular birefringence $\Omega=aI_B+\Omega_0$ and the linear dichroism, A. Here, we assume that the circular birefringence is a linear function of the applied current I_B, with Ω_0 an offset due to stray magnetic fields. Note the excellent agreement between the fit curve and the experimental data.

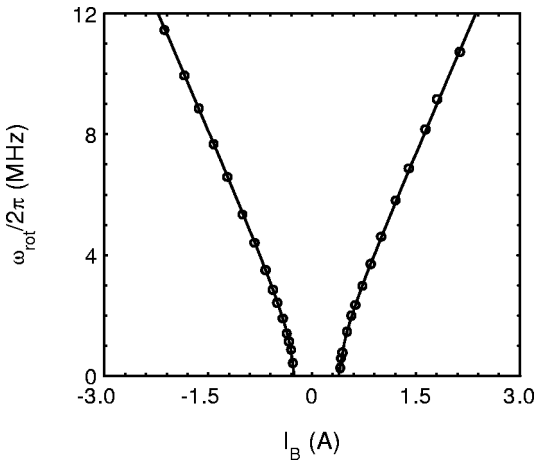

FIG. 5. Intensity-modulation frequency due to the polarization rotation as a function of the magnetic field; the points are the experimental data, the solid curve represents the theory. These data are used to determine *in situ* the value of the circular birefringence, Ω, as function of the applied current, I_B, and the linear dichroism, A. From the fit we find $a/2\pi=2.64$ MHz per Ampère, $A/2\pi=0.89$ MHz, and $\Omega_0/2\pi=-0.19$ MHz (see text).

B. Steady-state polarization

Next we measured the steady-state polarization angle of the laser light as function of the current through the magnetic coils in the locked regime ($|\Omega|<A$). The data in Fig. 6 were taken using the same set-up as for Fig. 5.

The behavior of the polarization angle of the lasing mode as function of the magnetic field is described by Eq. (12b). This is indicated by the solid curve in Fig. 6, where we used the values of a, Ω_0, and A as determined from the fit in Fig. 5. Clearly, the steady-state polarization of the laser behaves as predicted by theory.

C. Polarization noise

As is clear from Eqs. (15), the origin of the excess intensity and phase noise lies in the fluctuations of the polarization angle θ and the ellipticity χ, respectively. To measure the latter fluctuations, we use polarization optics that convert the polarization noise into intensity noise, which is detected (see Fig. 3). To measure polarization-angle noise, we use a polarizer with its transmission axis under 45° with respect to the steady-state polarization of the laser output. For this choice of angle the polarization-angle noise is maximally converted into intensity noise (see Appendix).

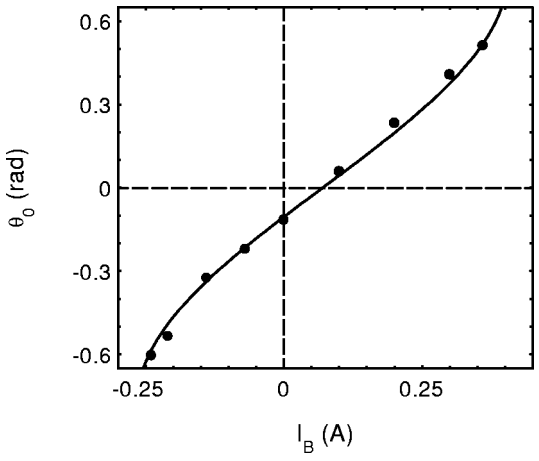

FIG. 6. Steady-state polarization angle of the lasing mode θ_0, as a function of I_B, the current generating the magnetic field. The points are experimental data, the solid curve is the theoretical prediction, Eq. (12b).

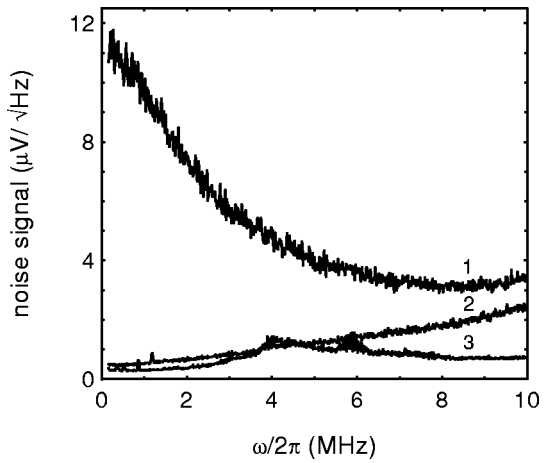

FIG. 7. Curve 1 represents the noise signal containing the polarization noise. Curve 2 is the result when only the intensity noise of the beam is measured; the curve is scaled to the amount of intensity noise in curve 1. Curve 3 gives the noise signal when no light falls onto the detector. Curve 1 shows the frequency dependence of the polarization dynamics.

In order to measure the ellipticity noise, we introduce a quarter-wave plate before the polarizer. The quarter-wave plate has its axes at 45° with respect to the steady-state polarization of the laser output, while the polarizer is set parallel to this polarization direction. This combination transmits only one circularly polarized component of the laser output. Since fluctuations in the amplitude of a circular component are responsible for the ellipticity fluctuations, the ellipticity fluctuations are converted into intensity noise by this configuration (see Appendix). In fact, it is not necessary to remove the quarter-wave plate when switching from ellipticity-noise to polarization-angle-noise measurement. For the polarization-angle noise measurement, the transmission axis of the polarizer is simply aligned with the fast/slow axis of the quarter-wave plate so that the quarter-wave plate has no effect.

Apart from the converted polarization noise, the noise signal detected after these polarization elements still contains the intrinsic intensity noise [see Eqs. (A1 and A2)]. In our experiments the relaxation oscillations were at a higher frequency than the polarization dynamics, so that the polarization-noise contribution in the signal after the polarizer was considerably larger in magnitude than the intrinsic intensity-noise contribution. To demonstrate this, the magnitude of the various noise signals is shown in Fig. 7. This data was taken under same conditions as Fig. 5, for $\Omega=0$. Curve 1 is the ''raw'' intensity noise signal after the polarizer. It contains the polarization-angle fluctuations, the intrinsic intensity fluctuations and the detector noise. Curve 3 shows the

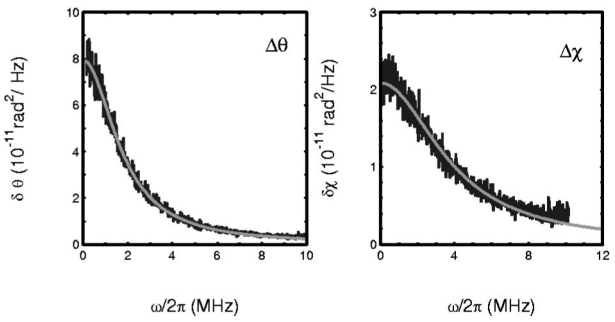

FIG. 8. Polarization-angle noise spectrum ($\delta\theta$) and ellipticity noise spectrum ($\delta\chi$) for $\Omega=0$ MHz; these spectra were corrected for the intensity noise and detector noise contribution by the method described in the text; see also Fig. 7. The curves through the experimental data are Lorentzian fits, yielding a width of the polarization-angle noise spectrum $\Delta\omega_{1/2}/2\pi=1.76$ MHz, and of the ellipticity noise spectrum $\Delta\omega_{1/2}/2\pi=3.59$ MHz.

noise signal when no light falls on the detector; this is the intrinsic noise of our detector-amplifier combination. Curve 2 represents the amount of intrinsic intensity noise present in curve 1. This curve was obtained by aligning the polarizer and the quarter-wave plate with the laser polarization (see Sec. IV D) to measure the intensity noise in isolation. As a next step, the detector noise signal (see curve 3) was quadratically subtracted from this signal and the result was scaled down by the ratio of its output power and the output power of curve 1 [about a factor of 2, cf. Eq. (A1)], leading to curve 2. The prominent peak at low frequencies (<4 MHz) of curve 1 shows that the polarization dynamics is spectrally well resolved, as the intrinsic intensity noise and detector noise are much less. At high frequencies (>8 MHz) the intrinsic intensity noise also becomes important due to the presence of relaxation oscillations.

We extracted the noise spectra of the polarization angle and the ellipticity by subtracting quadratically the intensity and detector noise [26]. Figure 8 shows an example of corrected spectra of the polarization-orientation noise and of the ellipticity noise at $\Omega=0$. The spectra in this figure are Lorentzians as expected from theory [see Eq. (15)], the width of the Lorentzian fit to the polarization-orientation noise spectrum is smaller than that to the ellipticity noise data. The widths of these Lorentzian curves yield information about the polarization dynamics, since they correspond to the relaxation rates towards the steady polarization state. Theoretically, for the polarization-angle noise the width at half maximum is expected to be $\Delta\omega_{1/2}=\gamma=2\sqrt{A^2-\Omega^2}$, which is the difference in loss between the two polarization modes. The value found from the fit $\gamma/2\pi=1.76$ MHz agrees very well with Fig. 5 where we found $A/\pi=1.78$ MHz. The width of the ellipticity fluctuations spectrum contains as an extra term the anisotropic saturation, $\Delta\omega_{1/2}=\gamma+2\beta_a I_0$. This explains the larger width at half maximum for the ellipticity noise in Fig. 8.

Figure 9 shows the measured width of the polarization noise spectra, $\delta\theta$ and $\delta\chi$, as a function of Ω/A; the cavity parameters were the same as for Fig. 5. It is seen that the width of the spectra gets smaller as the magnetic field (Ω)

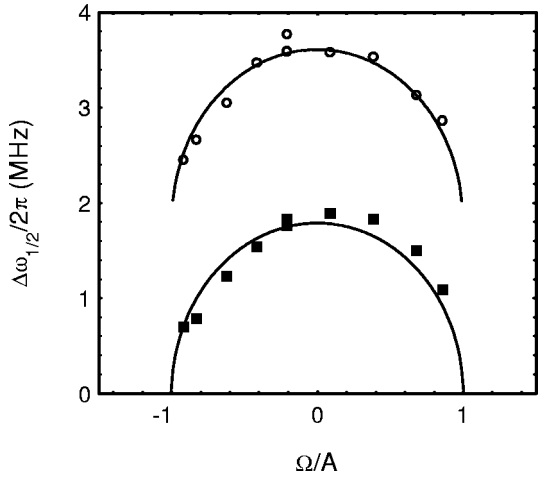

FIG. 9. Width of the polarization-noise spectra as function Ω/A. The squares are the experimental data of the polarization-angle noise, the circles are the experimental data of the ellipticity noise. The curves are theoretical; the curve through the polarization-angle noise data has no fit parameter. The curve through the ellipticity data contains one fit parameter, namely the strength of the anisotropic part of the polarization saturation. The horizontal solid line is a fit to the polarization-angle noise data, see text.

gets larger. In other words, the polarization dynamics gets slower as $|\Omega|/A$ approaches 1, as is expected from Eqs. (14). It is also obvious that the widths of the ellipticity-fluctuation spectra are shifted by an offset. We attribute this shift to the polarization anisotropic saturation, $\beta_a I_0$ [cf. Eq. (15d)]. The curves in Fig. 9 are based on Eqs. (15b) and (15d) using the parameters a, Ω_0, and A as determined from the measurement of the rotation frequency (Sec. IV A). The curve describing the ellipticity noise contains a fit parameter, namely the offset ascribed to the anisotropic polarization saturation; we obtain a value of $2\beta_a I_0=1.83$ MHz.

We have measured the power dependence of the shift $2\beta_a I_0$ at zero magnetic field ($\Omega=0$). The result is plotted in Fig. 10. This figure shows that whereas the width of the ellipticity noise spectrum increases linearly with the power, the width of the polarization-angle noise spectrum is independent of the power, as expected. The horizontal solid line is a fit to the polarization-angle noise data points, its height $\gamma/2\pi=1.94$ MHz corresponds excellently with the calibrated value of the linear dichroism, which in this case was $2A/2\pi=1.94$ MHz. From the linear dependence on the output power we determine the anisotropic saturation coefficient, $\beta_a=17\pm10$ kHz/μW. The error in our estimate of β_a is so large because β_a varied significantly from measurement to measurement, we attribute this to fluctuations in laser alignment and in gas composition (due to the Xe clean-up effect [27]).

Not only the width of the noise spectra, but also the total power contained in the noise spectra contains information. The ratio of the ac noise power and the dc laser output when measuring the polarization noise specifies the mean excursion from the steady-state polarization via $\langle\Delta\theta^2\rangle=\int_0^\infty\langle|\delta\theta(\nu)|^2\rangle d\nu$. Using the area under the curves in Fig. 8, we can calculate the mean excursion of the polarization

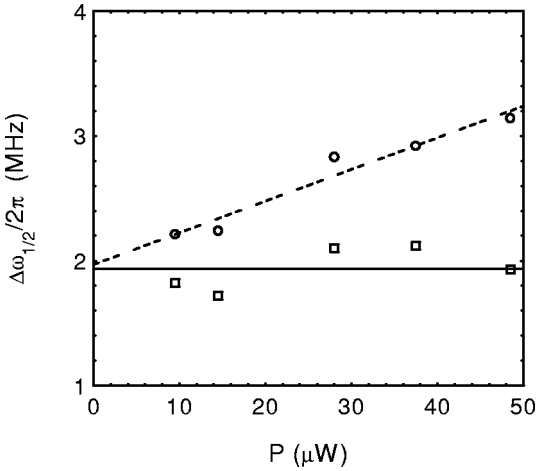

FIG. 10. Width of the ellipticity noise spectra (circles) and polarization-angle noise spectra (squares) plotted as function of the output power. The dashed line is a fit through the ellipticity noise data points, the slope of this curve gives the anisotropic saturation.

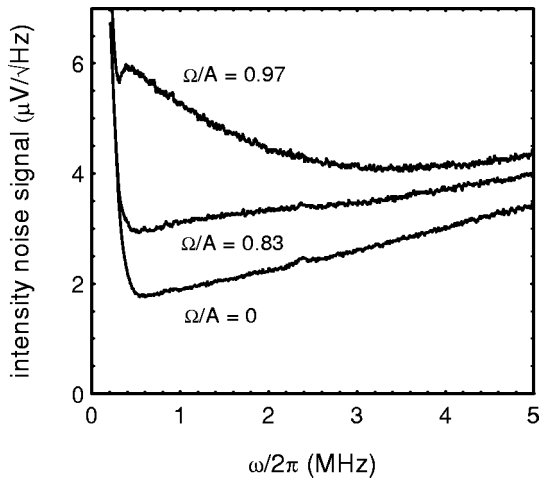

FIG. 11. Intensity-noise spectra for different values of the magnetic field. The extra noise contribution arising when the magnetic field (i.e., Ω) is increased is clearly visible at low frequencies.

angle from steady state. In the case of zero magnetic field, this leads to the value of $\sqrt{\langle \Delta\theta^2 \rangle} = 15$ mrad and $\sqrt{\langle \Delta\chi^2 \rangle} = 11$ mrad. As the magnetic field is increased these excursion angles get larger, proportional to γ^{-1}. In the experiments the value of γ decreased maximally by a factor of 5, so that the polarization fluctuations remain relatively small and the linearization approach still holds.

D. Intensity noise

The simplest way to measure the intensity noise of the laser is by removing all the polarization-sensitive elements between the laser and the detector, including the optical isolator. We verified with a rotatable half-wave plate placed just after the laser outcoupling mirror that no hidden polarization sensitive elements were left between the laser mirror and the InSb detector. A disadvantage of this measurement scheme is that, as the optical isolator was taken away, careful alignment was necessary to prevent optical feedback from the InSb detector back into the laser. Another way to detect the intensity noise signal is by having the polarization of the laser output parallel to the transmission axis of the polarizer. Here the disadvantage is that the signal is sensitive to misorientation of the polarizer. We have checked that both methods yielded the same result. The first method is more convenient in experiments where the steady-state polarization is changed and we used it to measure the excess intensity noise as function of the magnetic field. We used the second method when studying the correlations of polarization-angle noise and intensity noise as we already needed a polarizer to demonstrate the correlations in the first place.

In Fig. 11 intensity-noise spectra are depicted for different values of the magnetic field. This figure shows that the intensity noise increases as the magnetic field gets larger and that this extra noise is frequency dependent. At low frequencies the excess noise signal is higher than at high frequencies. As an aside, we note that the divergence in the spectrum around zero frequency is due to the zero-frequency peak of the spectrum analyzer convoluted with the resolution bandwidth of the spectrum analyzer. Although the resolution bandwidth is only 100 kHz in this case, the divergence still affects the curve from $\Omega = 0$ up to roughly 0.5 MHz since the intensity noise represents such a weak signal here.

In order to extract from the intensity noise spectrum the excess noise contribution (the extra noise caused by the nonorthogonality of the modes), we quadratically subtract the detector noise and normalize the intensity noise spectrum for the nonorthogonal modes ($|\Omega| > 0$) with respect to the intensity noise spectrum for orthogonal modes ($\Omega = 0$). This is plotted in Fig. 12. This figure shows that for high frequencies the excess noise is almost absent whereas it is strongest for

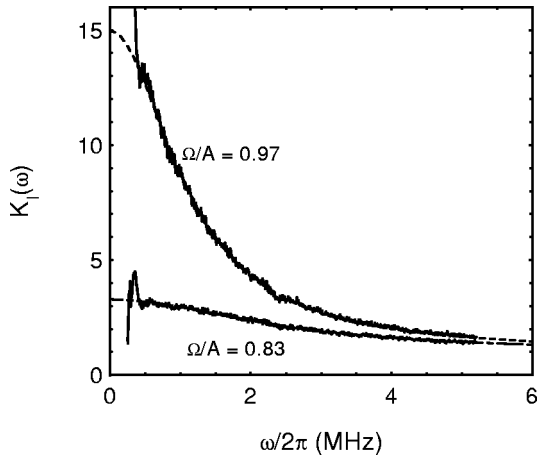

FIG. 12. The normalized intensity noise spectra of Fig. 11 emphasizing the enhancement of the noise due to the nonorthogonality of the cavity modes. This graph shows clearly that the excess noise is frequency dependent. At high frequencies the excess noise factor approaches unity whereas at low frequencies it attains its maximum value. Dashed curves are the Lorentzain fits. From these fits we find $A/2\pi = 2.2(1)$ MHz, and $\Omega/A = 0.83$ and $\Omega/A = 0.97$, respectively, which agree very well with the polarization-rotation calibration, namely: $A/2\pi = 2.1(1)$ MHz and $\Omega/A = 0.83(2)$ and $\Omega/A = 0.97(2)$, respectively.

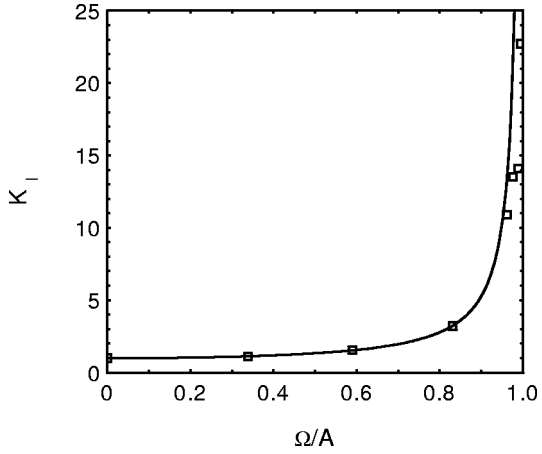

FIG. 13. Excess noise at low frequencies as function of the nonorthogonality; the solid curve is the theoretical expectation based on the linear mode analysis.

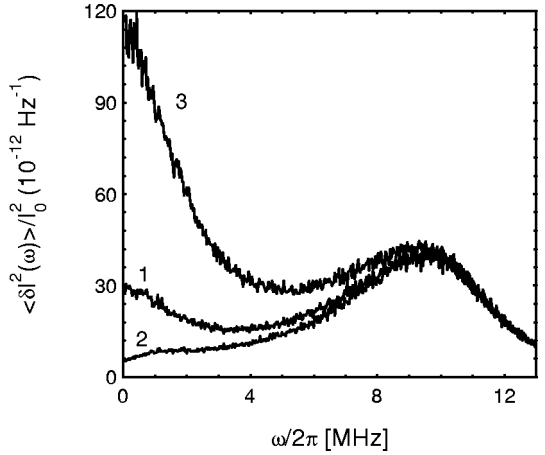

FIG. 14. Intensity noise measured after a polarizer for different angles of the polarizer. Curve 1: the polarizer transmission axis is aligned with the polarization of the laser, this curve is equal to the intrinsic intensity noise. Curve 2: the polarizer is rotated by 15° in one direction, the correlation between the intensity noise and the polarization-angle noise is seen in the reduction of the noise signal. Curve 3: the polarizer is rotated by 15° in the other direction.

low frequencies, i.e. the excess noise is colored; this corresponds to dynamics in the time domain [14]. The deviation of the excess quantum noise in the experimental data at very low frequencies is due to the effect of the divergence at zero frequency. The dashed curves in Fig. 12 are fits to the normalized intensity noise spectra using Eq. (15a). The fit values obtained for Ω and A are in excellent agreement with those obtained from the polarization rotation calibration.

In the linear mode analysis, in which the excess noise follows from the eigenmode nonorthogonality, the dynamics is neglected (Sec. II A). In our measured spectra this corresponds to looking at the excess noise at low frequencies. To verify this interpretation, we have extracted the excess noise factor at low frequencies (0.5 MHz) from curves as depicted in Fig. 12. The result is plotted in Fig. 13 as function of Ω/A. The observed enhancement at low frequencies is in good agreement with the theoretical expectation, which is drawn in this figure as the solid line $[K_I=1/(1-|\Omega/A|^2)]$. We can explain the deviation at higher values of Ω/A as a consequence of the fact that the enhancement was taken at around 0.5 MHz (instead of at zero frequency).

E. Correlations between intensity noise and polarization-angle noise

The polarization mode-nonorthogonality not only introduces excess intensity noise, but also gives rise to correlations between the intensity noise and the polarization-angle noise [see Eq. (18)]. We verified the existence of the correlations by mixing the polarization-angle fluctuations into the intensity noise. This was conveniently done in our setup by placing a rotatable polarizer in the laser output. By changing the angle between the transmission axis of the polarizer and the steady-state polarization of the laser output, we control the magnitude of polarization-angle noise that is mixed in [see Eq. (A1)].

In Fig. 14, the resulting noise spectra are shown for three angles of the polarizer. The experimental conditions for these curves were: $\Omega/A=0.98(2)$, $A/2\pi=2.5(1)$ MHz and $P_{out}=26$ μW. The bump around 10 MHz in the spectra corresponds to the relaxation oscillations of the laser. Curve 1 is taken when the orientation of the polarizer is aligned with the steady-state polarization of the laser light. As noted before, we verified that this case is identical to the intrinsic intensity noise spectrum measured without a polarizer. Curve 2 gives the spectrum when the polarizer is rotated by 15° in one direction; this angle was chosen to minimize the observed noise at low frequencies. The fact that the observed noise is less than for the first case, proves the existence of correlations between polarization-angle and intensity noise: if the polarization noise and intensity noise would have been uncorrelated, adding the extra noise could only result in increased total noise. Curve 3 shows the case when the polarizer is rotated from the position corresponding to curve 1 by 15° in the *other* direction. In this case the polarization-orientation noise is mixed ''in phase'' and the total amount of excess noise power increases with about a factor of 4, as expected.

To quantify the strength of the correlations we took as a measure the angle of the polarizer (with respect to the polarization of the laser output) for which the low-frequency noise is suppressed most. The resulting angles are plotted in Fig. 15 as a function of the magnetic field for three different output powers ($P_{out}=40$ μW, $P_{out}=25$ μW, and $P_{out}=13$ μW, respectively). The figure shows that the strength of the correlation increases as Ω (i.e., the magnetic field) increases. This is to be expected as the correlations increase as the nonorthogonality increases [see Eq. (18)]. Furthermore the figure shows that the strength of the correlations decreases as the output power gets higher. The solid lines are linear fits through the experimental data. The variation in the slope of the curves in Fig. 15 is due to the different output powers used. From the output power dependence of these slopes (see inset of Fig. 15), a value for the isotropic saturation can be derived [see Eq. (A4)], yielding $\beta_i=0.6\pm0.2$ MHz/μW.

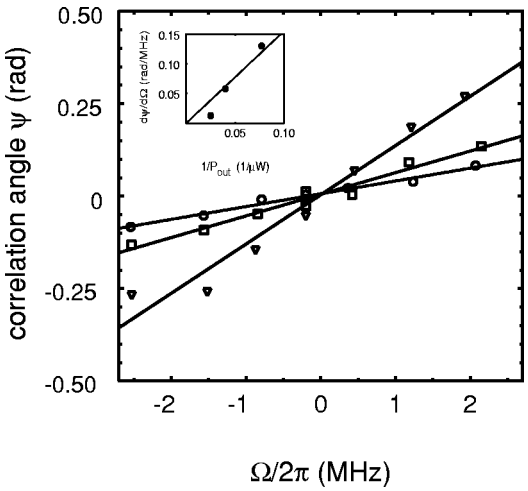

FIG. 15. Angle ψ of the polarizer for minimal intensity noise after the polarizer as function of the magnetic field, for different output powers. ○, $P_{\mathrm{out}}=40\ \mu$W; □, $P_{\mathrm{out}}=25\ \mu$W; ▽, $P_{\mathrm{out}}=13\ \mu$W. The figure shows that the strength of the correlations is proportional to the magnetic field and inversely proportional to the output power. The three sets of data points are fitted with straight lines. The insert shows the slopes of the lines in the main figure versus the inverse output power P_{out}^{-1}. The fitted straight line through those points allows us to determine β_i.

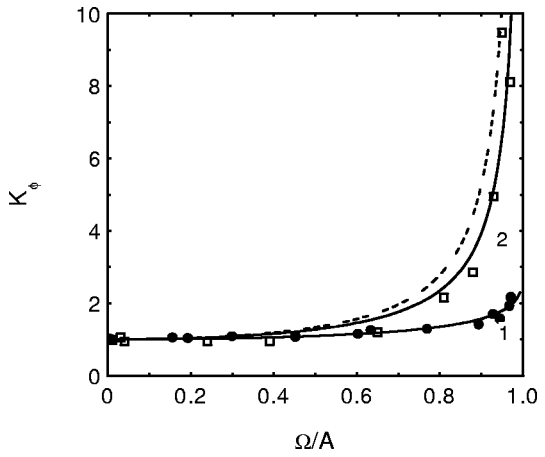

FIG. 16. Excess noise factors in the optical linewidth of the laser as a function of the magnetic field for two different output powers. The circles are experimental data with $A/2\pi=0.61$ MHz at an output power of 35 μW. The squares are experimental points with $A/2\pi=2.32$ MHz at an output power of 9 μW . Curves 1 and 2 are theoretical curves according to Eq. (17) for the corresponding output powers. Dashed curve : K_ϕ following from the linear mode analysis (no polarization-anisotropic saturation).

F. Phase noise

We now discuss the last laser parameter described in Sec. II, namely the optical phase ϕ [see Eq. 15c]. As described in Sec. II B, ellipticity fluctuations are coupled into the phase noise, similar to the coupling of polarization-angle fluctuations into the intensity noise. However, in contrast to the excess intensity noise, the excess phase noise is affected by the anisotropic saturation as already discussed in Sec. II; it is expected to decrease as a function of laser output power. The decrease will depend on the ratio $\beta_a I_0/A$. In order to make this decrease visible, we measured the phase noise at a high power and a weak dichroism ($P_{\mathrm{out}}=35\ \mu$W and $A/2\pi=0.61$ MHz) and at low power and strong dichroism ($P_{\mathrm{out}}=9\ \mu$W and $A/2\pi=2.32$ MHz). To detect the quantum phase fluctuations we used a self-heterodyne set-up (Sec. III), and measured the phase linewidth of the laser as function of the magnetic field. The value at zero magnetic field gives the reference value for orthogonal polarization modes (typically this corresponded to a linewidth in the range of 0.5 kHz–4 kHz). The excess noise factor of the optical phase, K_ϕ, follows from dividing the linewidth at nonzero magnetic fields by this value. This is plotted in Fig. 16. The solid curves are theoretical curves based on the output power and the value of the anisotropic saturation as determined in Sec. IV C [$\beta_a=17(10)$ kHz/μW]. Note the excellent agreement with the theoretical curves, which are based on the independent ellipticity-noise data, without any free parameter. Figure 16 clearly shows the effect of the polarization-anisotropic saturation; for high output power the excess noise factor for the optical phase stays nearly the same as the magnetic field is increased, whereas for low power the excess quantum noise is hardly suppressed. This proves that the linear mode analysis gives a wrong result for the excess phase noise of the laser, the nonlinearity of the gain medium (specifically: the polarization-anisotropic saturation) can *not* be neglected.

V. CONCLUDING DISCUSSION

We have examined the quantum-noise properties of a HeXe gas laser both theoretically and experimentally, as function of the nonorthogonality of the polarization modes of the cavity. Theoretically, we have extended the usual approach to excess quantum noise (namely a linear mode analysis of the laser) to a model that explicitly includes the gain saturation, taking into account both the isotropic and anisotropic part thereof. Because the extended model is nonlinear, the usual approach in the linear mode analysis to obtain excess noise factors, cannot be used. Instead, we have expanded the equations around the stable lasing mode to show how fluctuations in the polarization degrees of freedom (i.e., noise in the nonlasing mode) leads to excess noise in the intensity and the phase (i.e., noise in the lasing mode). Specifically, we find that in our case the polarization-angle fluctuations couple into the intensity noise and that the ellipticity fluctuations couple into the phase noise.

The model also contains the noise dynamics, which is usually lost after projection in the linear mode analysis. When the noise dynamics is negligible, i.e., at low frequencies, the extended model predicts the same excess intensity noise as the linear mode analysis. Frequency-resolved measurements of the intensity noise confirm the predicted magnitude of the excess noise and show the dynamics of the excess quantum noise, i.e., its coloring. The frequency bandwidth of the excess quantum noise is a few MHz, i.e., a much slower timescale than the cavity round-trip time ($\sim$1 ns). This is a striking example of the fact that the excess quantum noise takes usually many roundtrips to build up. The coupling of the polarization-angle fluctuations and inten-

sity fluctuations introduced by the nonorthogonality of the polarization modes is also demonstrated by the experimental verification of the correlation between these two.

The influence of the polarization-anisotropic saturation shows itself in the ellipticity fluctuations. Measured spectra confirm that the damping rate of the ellipticity fluctuations is faster due to the anisotropic saturation. This nonlinear mechanism cannot be taken into account in a linear mode analysis, and the observed excess phase noise is less than the linear prediction. Experimentally, we measured that excess phase noise is suppressed more for higher output powers, which confirms the role of the polarization-anisotropic saturation. This shows that the excess noise factor for the phase can differ from the excess noise factor for the intensity.

From the power dependence of the strength of the correlations and the power dependence of the width of the ellipticity-noise spectrum we can determine the ratio of the polarization isotropic saturation and the polarization anisotropic saturation; this yields $\beta_a/\beta_i=0.028$. For a laser without pressure broadening the theory based on the coupling of the atomic levels due to the light field yields $\beta_a/\beta_i=0.4$ for $J=3$ to $J=2$ transitions [23]. Intuitively, one would expect the collisions to randomize the Zeeman sublevel populations, reducing the ratio β_a/β_i by a factor $\gamma_{\rm nat}/\gamma_{\rm coll}\simeq 0.03$, where $\gamma_{\rm nat}$ is the natural linewidth ($\simeq 5$ MHz) and $\gamma_{\rm coll}$ is the pressure broadening ($\simeq 150$ MHz at 2 kPa) [28], leading to $\beta_a/\beta_i=0.012$. The coincidence with the experimental value $\beta_a/\beta_i=0.028$ is within the same magnitude but may be fortuitous.

In theory the excess-noise factor diverges when $\Omega/A \rightarrow 1$; in the experiment we observed maximum enhancements of 50. One reason for this is that a high stability of the set up is required for high K factors; reaching $K_{\rm pol}=50$, requires $\Omega/A=0.99$, so accuracies of better than one percent are needed to achieve higher K values. Another point is that when $|\Omega|/A\rightarrow 1$ the influence of small, unintentional birefringence (for instance due to strain in the capillary windows) will influence the mode nonorthogonality and limit the maximum enhancement. If these technical limitations could be overcome, the next limit would probably be that the excess quantum noise is no longer small enough to validate a linearized description of its effect. It would be interesting to study the noise properties of a device with this kind of giant excess quantum noise.

It would also be interesting to see how far the insights obtained here can be extended to nonorthogonal *transverse* modes. Unstable resonators are known to have nonorthogonal transverse modes and can have very large excess noise factors [5,6]. The unstable resonator, however, is much more complicated than the polarization mode case due to presence of many more transverse modes than the two polarization modes. A two-mode approximation does not describe the observed excess noise factors quantitatively [10]. Our results point to the important role of the nonlinearity of the saturation. For instance, the anisotropic saturation of the gain medium can significantly modify the observed excess noise factor. So far, such anisotropy has not been taken into account in the calculation of excess noise for nonorthogonal transverse modes [4,8,11] and it is completely unknown to what extent it plays a role in that case. We also found the isotropic saturation (β_i) to be important for a quantitative analysis of the power dependence of the excess noise, in particular for the observed correlations between intensity and polarization-angle noise (cf. Fig 15). Again a linear mode analysis cannot describe this power dependence. Furthermore, it would be interesting to explicitly demonstrate the coloring of excess noise for nonorthogonal transverse modes.

Summarizing, the measured spectra of noise in the polarization parameters, intensity and optical phase of the laser are in excellent agreement with a model including the nonlinearity and anisotropy of the gain saturation. In contrast, the linear mode description only gives good results for the enhancement in the intensity noise. For the phase noise the anisotropic saturation of the gain medium directly affects the observed excess noise factor.

ACKNOWLEDGMENTS

We acknowledge support of the Stichting voor Fundamenteel Onderzoek der Materie (FOM) which is supported by NWO. The research of N. J. van Druten has been made possible by the ''Koninklijke Nederlandse Akademie van Wetenschappen.'' We also acknowledge support from the European Union under TMR Contract No. ERB4061PL95-1021 (Microlasers and Cavity QED).

APPENDIX: NOISE SIGNAL AFTER A POLARIZER

In this appendix we will briefly derive the expressions for the noise signal after several polarization elements. We take the x axis along the polarization direction of the laser, so that the field of the laser output in the x,y linearly polarized basis is described by

$$\vec{E}=\begin{pmatrix} E_0+\delta E_x \\ \delta E_y \end{pmatrix}.$$

With this definition, and linearizing around steady state, the polarization-angle fluctuations are $\delta\theta\approx\delta E_y/E_0$ and the intensity fluctuations are $\delta I=(E_0+\delta E_x)^2+\delta E_y^2-E_0^2 \approx 2E_0\delta E_x$. A polarizer is inserted with an angle ψ between the transmission axis of the polarizer and the x axis. In first-order approximation of small fluctuations the signal after the polarizer is:

$$I_{\rm after}\approx(I_0+\delta I)\cos^2\psi+I_0\sin 2\psi\,\delta\theta. \qquad \text{(A1)}$$

The equation shows that when $\psi=0$ the signal after the polarizer does not contain any polarization-angle noise so that only the intensity noise signal will be measured. When $\psi=45°$ and $\sin 2\psi=1$ the polarization-noise signal will be maximal. In this case, the signal is $I_{\rm after}=(I_0+\delta I)/2+I_0\delta\theta$. Note that the signal not only contains polarization-angle noise, but also a contribution of the intensity noise of the original laser output.

To detect the ellipticity noise we use a combination of a quarter-wave plate and a polarizer such that only one circularly polarized component (taken here to be I_+) is transmitted. The resulting signal is

$$I_{\text{after}} = I_+ + \delta I_+ = \frac{1}{2}(I_0 + \delta I + 2I_0 \delta\chi). \tag{A2}$$

Again, apart from the ellipticity noise a contribution of the intrinsic intensity noise is still present.

The spectra detected are the power spectra of the intensity noise after the polarization elements $\langle |I_{\text{after}}(\omega)|^2 \rangle$. These contain the sum of the intensity and polarization-noise contributions. The polarization noise without the intensity noise contribution is obtained by subtracting the intrinsic intensity noise quadratically from the total spectrum [26].

In order to measure the strength of the correlations between the intensity and the polarization angle we want to find the angle ψ that minimizes the noise after the polarization elements. It is useful to write the intrinsic intensity noise in the laser output as a sum of two terms, one that depends on the polarization-angle fluctuations, and another that is independent of the polarization-angle fluctuations. Taking the Fourier transform of Eqs. (14) and setting the frequency $\omega = 0$, yields the desired separation,

$$\delta I = 2I_0 \delta\tilde{I} = 2I_0 \left(\frac{f_{\tilde{I}}}{2\beta_i I_0} - \frac{\Omega \delta\theta}{\beta_i I_0} \right). \tag{A3}$$

When polarization noise is mixed into the intrinsic intensity noise by a polarizer, this can act to compensate the part of the intensity noise that originates from polarization-angle fluctuations. Combining Eq. (A3) with Eq. (A1) yields the angle $\psi_{\min}$ for which the polarization-angle fluctuations in the intrinsic intensity noise are compensated for after the polarizer,

$$\psi_{\min} \approx -\frac{\Omega}{\beta_i I_0}. \tag{A4}$$

[1] A. E. Siegman, Appl. Phys. B: Lasers Opt. **60**, 247 (1995).
[2] A. L. Schawlow and C. H. Townes, Phys. Rev. **112**, 1940 (1958).
[3] K. Petermann, IEEE J. Quantum Electron. **QE-15**, 566 (1979).
[4] A. E. Siegman, Phys. Rev. A **39**, 1253 (1989); **39**, 1264 (1989).
[5] Y.-J. Cheng, C. G. Fanning, and A. E. Siegman, Phys. Rev. Lett. **77**, 627 (1996).
[6] M. A. van Eijkelenborg, Å. M. Lindberg, M. S. Thijssen, and J. P. Woerdman, Phys. Rev. Lett. **77**, 4314 (1996).
[7] P. Grangier and J.-P. Poizat, Eur. Phys. J. D **1**, 97 (1998).
[8] P. Grangier and J.-P. Poizat, Eur. Phys. J. D **7**, 99 (1999).
[9] O. Emile, M. Brunel, F. Bretenaker, and A. Le Floch, Phys. Rev. A **57**, 4889 (1998).
[10] Å. M. Lindberg, M. A. van Eijkelenborg, K. Joosten, G. Nienhuis, and J. P. Woerdman, Phys. Rev. A **57**, 3036 (1998).
[11] G. H. C. New, J. Mod. Opt. **42**, 799 (1995).
[12] G. P. Karman, Å. M. Lindberg, and J. P. Woerdman, Opt. Lett. **23**, 1698 (1998).
[13] A. M. van der Lee, N. J. van Druten, A. L. Mieremet, M. A. van Eijkelenborg, Å. M. Lindberg, M. P. van Exter, and J. P. Woerdman, Phys. Rev. Lett. **79**, 4357 (1997).
[14] A. M. van der Lee, M. P. van Exter, A. L. Mieremet, N. J. van Druten, and J. P. Woerdman, Phys. Rev. Lett. **81**, 5121 (1998).
[15] O. Emile, M. Brunel, A. Le Floch, and F. Bretenaker, Europhys. Lett. **43**, 153 (1998).
[16] Y. Yamamoto, *Coherence, Amplification, and Quantum Effects in Semiconductor Lasers* (Wiley, New York, 1991), Chap. 11.
[17] W. W. Chow, J. Gea-Banacloche, L. M. Pedrotti, V. E. Sanders, W. Schleich, and M. O. Scully, Rev. Mod. Phys. **57**, 61 (1985).
[18] M. Born and E. Wolf, *Principles of Optics*, 6th ed. (Cambridge University Press, Cambridge, UK, 1998).
[19] M. Sargent III, M. O. Scully, and W. E. Lamb, Jr., *Laser Physics* (Addison-Wesley, Reading, MA, 1974).
[20] F. T. Arecchi, in *Instabilities and Chaos in Quantum Optics*, edited by F. T. Arrechi and R. G. Harrison (Springer-Verlag, Berlin, 1987).
[21] M. P. van Exter, R. F. M. Hendriks, and J. P. Woerdman, Phys. Rev. A **57**, 2080 (1998).
[22] M. P. van Exter, M. B. Willemsen, and J. P. Woerdman, Phys. Rev. A **58**, 4191 (1998).
[23] W. van Haeringen, Phys. Rev. **158**, 256 (1967).
[24] J. D. Cresser, W. H. Louisell, P. Meystre, W. Schleich, and M. O. Scully, Phys. Rev. A **25**, 2214 (1982); J. D. Cresser, D. Hammonds, W. H. Louisell, P. Meystre, and H. Risken, *ibid.* **25**, 2226 (1982); J. D. Cresser, *ibid.* **26**, 398 (1982).
[25] S. J. M. Kuppens, M. P. van Exter, and J. P. Woerdman, Phys. Rev. Lett. **72**, 3815 (1995).
[26] As is shown in the Appendix and Sec. IV E, correlations exist between the intensity noise and the polarization angle fluctuations for nonorthogonal eigenmodes; we neglect these correlations in this correction procedure as they have a minor effect on the polarization angle fluctuations.
[27] S. J. M. Kuppens, M. A. van Eijkelenborg, C. A. Schrama, M. P. van Exter, and J. P. Woerdman, IEEE J. Quantum Electron. **32**, 383 (1996).
[28] R. Vetter and E. Marié, J. Phys. B **11**, 2845 (1978).